AERODYNAMIC CHARACTERISTICS OF SPIN PHENOMENON FOR DELTA WING

Yoshiaki NAKAMURA (nakamura@nuae.nagoya-u.ac.jp)
Takafumi YAMADA (yamada@nuae.nagoya-u.ac.jp)
Department of Aerospace Engineering, Nagoya University
Nagoya, 464-8603, Japan

Abstract

The experiments of a delta wing's spinning phenomenon were conducted at the low speed wind tunnel of Nagoya University with the exit test section inclined vertically. The spin rate of the delta wing in the free rotation mode was measured as well as surface pressure distributions on the spinning delta wing. At low angles of attack the spin rate increases with sideslip angle, while near the stall angle, the opposite tendency appears. At low angles of attack, when the wing has a sideslip angle, the upper surface pressures on the windward wing-half become lower than those on the leeward wing-half. However, near the stall angle the upper surface pressures of the leeward wing-half become lower than those in the windward wing-half. These asymmetric pressure distribution patterns cause the spinning motion of the delta wing. From the pressure distributions and flow visualizations, it is evident that leading edge separation vortices play an important role in the spin phenomena. It is also found that at the equilibrium spin rate, where the wing rotates at a nearly constant angular velocity, the pressure difference between upper and lower surfaces, ΔC_p, shows a nearly symmetric distribution about the wing centerline.

Nomenclature

b:	span
b_x:	local span length at position x along the x-axis
c:	chord length
C_p:	pressure coefficient, $C_p = (p-p_\infty)/(1/2)\rho V^2$
ΔC_p:	pressure difference between upper and lower surfaces
$\Delta C_{p,L}$:	pressure difference between upper and lower surfaces on the leeward side
$\Delta C_{p,W}$:	pressure difference between upper and lower surfaces on the windward side
p:	measured pressure at taps
p_∞:	static pressure
R_e:	Reynolds number
S_p:	spin coefficient, $S_p = b\Omega/2V$
t:	wing thickness
V:	uniform flow velocity
v_t:	wing tip velocity
α:	angle of attack
$\alpha_{e,L}$, $\alpha_{e,W}$:	effective attack angle on the leeward and windward sides, respectively
β:	sideslip angle
τ:	wing thickness ratio, $\tau = t/c$
Λ:	swept-back angle
Λ_{eff}:	effective swept back angle
Ω:	rotating angular velocity

1. Introduction

Spin phenomena have been investigated for a long time[1)~7)], because they often cause serious accidents of aircraft. In those experiments, aircraft models with horizontal and vertical tails[8)], or an anti-spin fin[9)], have been used. However, it is difficult to apply the data on one aircraft to another aircraft, because they are valid for each airplane.

The objective of the present study is to examine fundamentals of aircraft spin characteristics. To make the analysis simple, only a main wing was chosen as a target.

In our previous study[10], aerodynamic characteristics of a flat plate wing were examined, and it was found that the asymmetric pattern of spanwise lift distribution causes the spin of the flat plate wing. In this study, a delta wing is chosen as another representative wing shape.

Here we consider the effects of yaw angle in addition to attack angle as spin parameters. In the cases of deep spin, i.e., α=10, 30 and 50 deg with a certain sideslip, surface pressure distributions were measured on a spinning delta wing, as well as the number of rotation. As they are scarcely available, these data seem to contribute to analyze the spin phenomena on aircraft.

2. Experimental facility and conditions

The present experiments used the wind tunnel of Nagoya University. The exit shape of the wind tunnel is a regular octagon with a diameter of 1980mm. One of features of this tunnel is its exit section that can be inclined from the horizontal direction to any arbitrary angle between –15 and 95 deg. In this study the angle was set to 90 deg, i.e., a vertical position.

Figure 1 shows the schematic of the facility. The model under consideration is a delta wing, which can rotate about a vertical axis. That is, the present system has one degree of freedom with regard to motion. The wing hangs from a shaft, which is fixed on a support with bearings. A motor is set on this support, which rotates the shaft through a gearbox. Thus, the wing is forced to rotate. The rotational velocity of the wing is controlled by an external D. C. power supply. On the other hand, when this driving mechanism is removed, the wing can rotate freely.

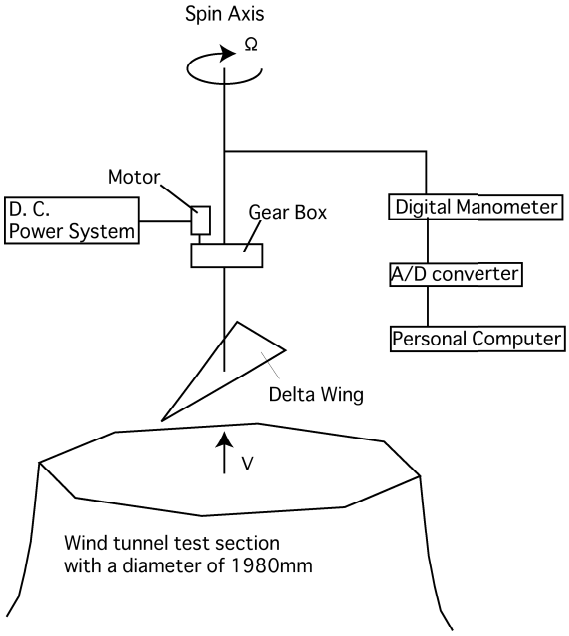

Fig.1 Schematic view of experimental facility

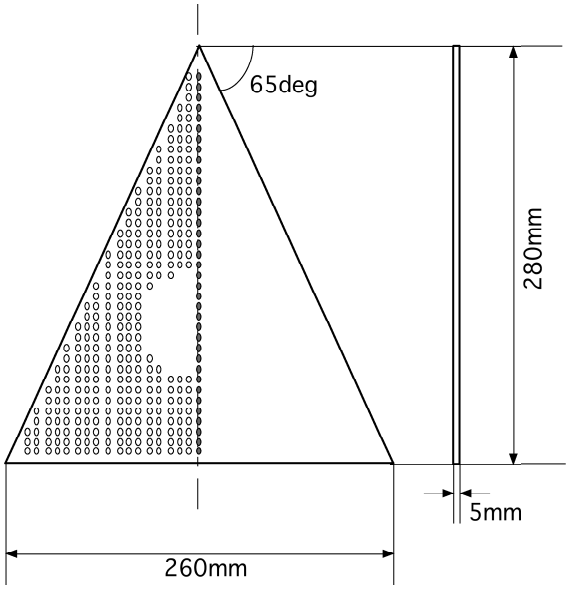

Fig.2 Configuration of delta wing

The wing employed here has a swept-back angle, Λ, of 65deg, a span length, b, of 260mm, a chord length, c, of 280mm, and a thickness ratio, τ, of 1.8%. The model has 290 pressure taps, which are located on the port side (see Fig. 2). These pressure taps are connected to an external digital manometer via stainless and silicon tubes.

Pressure was measured twenty times at intervals of 0.4 seconds for each pressure tap, the data of which were averaged. The standard deviation of

measurement errors is within 0.06mmAq.

Figure 3 shows the coordinate system used here. In the case of sideslipping, the wing-half on the forward side is referred to as the windward side, while that on the retreating side as the leeward side.

The non-dimensional spin rate, S_p, is defined by using Ω, b and V as S_p =bΩ/2V. In the present experiment, the free stream velocity is V= 10m/s, and the Reynolds number based on the chord length is R_e=1.7x10^5.

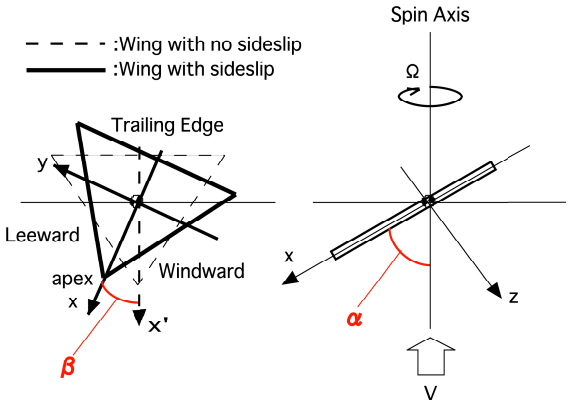

Fig. 3 Coordinate system employed here

In order to see the detailed flow field around the delta wing, flow visualization by a smoke wire method was also carried out. To perform the visualization, the flow speed of the wind tunnel was reduced to V=5m/s, and the model was lighted in the dark background, which was recorded by a digital video camera.

3. Results and discussion

3.1 Relation between sideslip angle and spin coefficient

To make clear the relation between sideslip angle β and spin coefficient S_p, the number of wing rotation was measured at α=10, 30 and 50deg with β as a parameter. These results are shown in Fig. 4.

In the case of α=10deg, S_p takes 0.1 at β =10deg, where the wing rotates clockwise at 60rpm, when viewed from upward. For this angle of attack, S_p takes positive values for β>0, while it takes negative values for β<0.

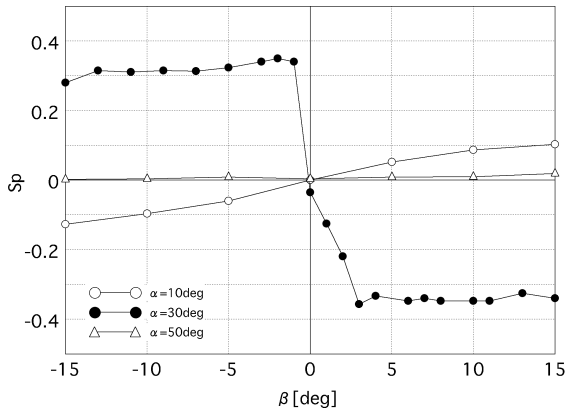

Fig. 4 Spin coefficient vs. sideslip angle

In the case of α=30deg, the characteristics are opposite to those of α=10deg. At β=10deg, S_p takes –0.35, where the wing rotates counterclockwise at 210rpm, and its magnitude is 3.5 times as large as that of α=10deg.

In the case of α=50deg, the characteristics are similar to the case of α=10deg. However, the wing rotation of the wing is negligible.

3.2 Relation between flow field around wing and spin coefficient

It is considered that the spin characteristics shown in Fig. 4 have been caused by the difference in flow field due to the wing attitude. To examine the relation between the flow field around the wing and the spin coefficient, pressure distribution measurements and flow visualization were carried out.

3.2.1 The case of α=10deg

Figure 5 shows the distributions of ΔC_p, i.e., the pressure difference between upper and lower wing surfaces, at α=10deg for β=0 and 10deg.

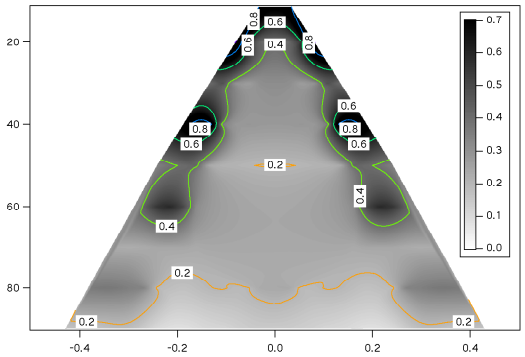

(a) α=10deg, β=0deg

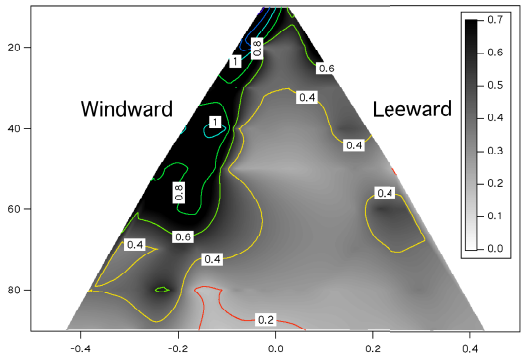

(b) α=10deg, β=10deg

Fig. 5 Contours of pressure difference between upper and lower wing surfaces

We can see from Fig. 5(a) that regions with large ΔC_p exist near the leading edge, and that the effects of aerodynamic force on the wing is symmetric about the wing center line (y=0). Therefore, this attitude will not produce any rotation of the wing.

On the other hand, at a sideslip angle, β, of 10deg, the values of ΔC_p on the windward side become larger than those on the leeward side. (see Fig. 5(b)) This asymmetric aerodynamic force distribution causes a clockwise rotation of the wing, when viewed from upward.

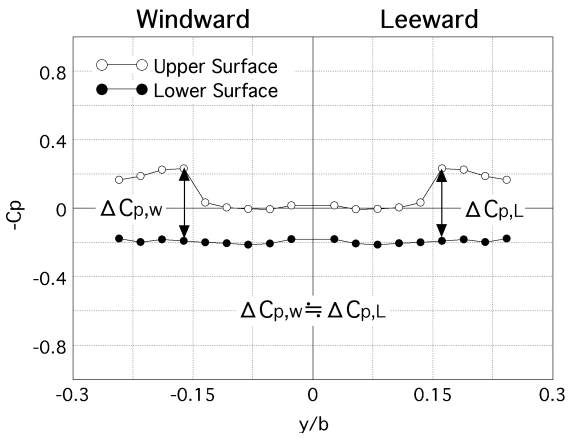

(a) β=0deg

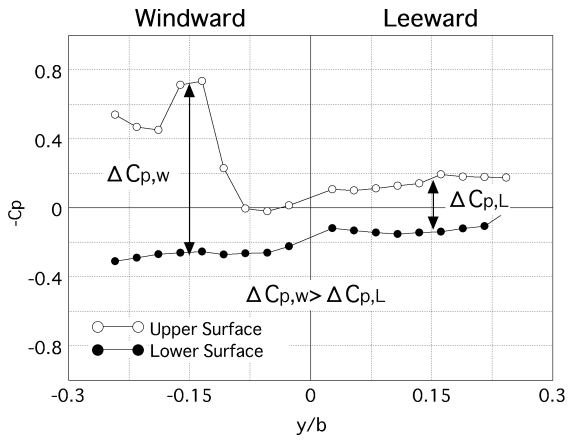

(b) β=10deg

Fig. 6 Spanwise pressure distributions at x/c=0.5 for α=10deg

Figure 6 shows the pressure distributions in the spanwise direction at x/c=0.5 on the upper and lower surfaces. In Fig. 6(a) symmetric low-pressure regions exist near both leading edges. This seems to be the effect of leading edge separation vortices generated from the wing apex.

On the other hand, by sideslipping, the pressures on the upper surface of windward wing-half become lower than those of the leeward wing-half. More specifically, compared with the case with no sideslipping, the pressures on the leeward side increase, while those on the windward side decrease.

In addition, sideslipping can increase the pressures on the lower surface of the windward wing-half,

while it can decrease the pressures on the lower surface. Thus, the effects of aerodynamic force on the wing become asymmetric about the wing centerline (y=0), which causes the wing to rotate.

If this asymmetric force distribution could be kept, the wing rotation would increase up to infinity. However, in fact, the wing continues to rotate at a certain equilibrium rotation number. To examine this mechanism, pressure measurements were performed for the rotating wing, the results of which are shown in Fig. 7.

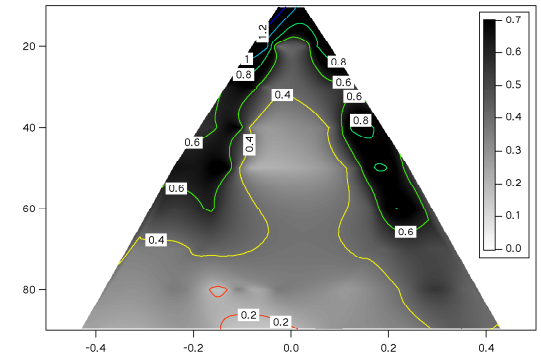

(a) Distribution of pressure difference between upper and lower wing surfaces

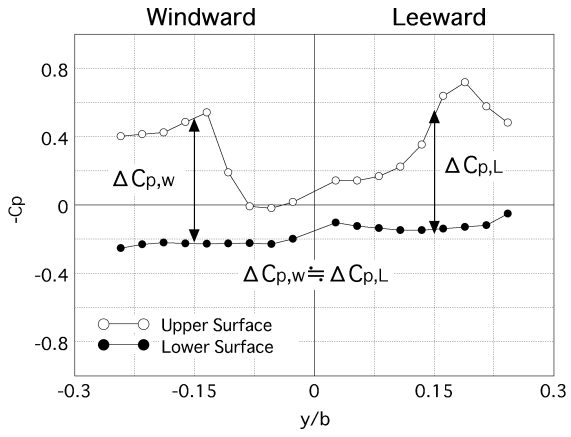

(b) Spanwise pressure distributions at x/c=0.5

Fig. 7 Characteristics of pressure distribution for the wing at an equilibrium rotation: α=10deg, β=10deg, and S_p=0.1

Figure 7(a) shows the distribution of ΔC_p at α=10deg, β=10deg, and S_p =0.1. Although a large ΔC_p region exists near the leading edge on the windward side around the apex, overall pressure distribution is nearly symmetric, compared with Fig. 5(b).

Figure 7(b) shows the pressure distribution on the upper and lower surfaces at x/c=0.5 when the wing is forced to rotate at S_p =0.1. The rotation increases the pressure on the upper surface of the windward side, and decreases those on the leeward side. Thus, the pressure distribution on the upper surface becomes nearly symmetric. The reason for this is described in the following.

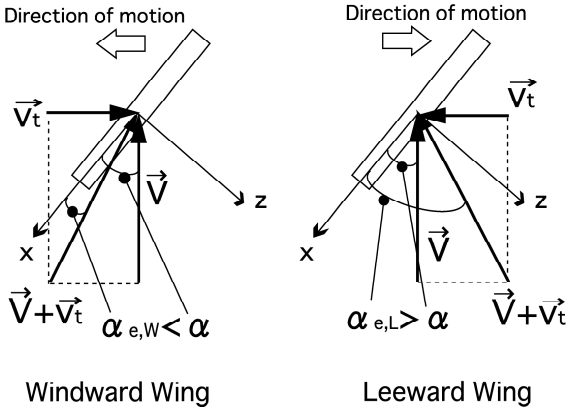

Fig. 8 Difference of effective attack angle between windward and leeward sides

When the wing is rotating, the relative angle of attack on the windward side is reduced, because it moves forward, while that on the leeward side is increased, because it moves backward (see Fig. 8).

On the windward side, the flow with v_t =(b_x/2)XΩ is relatively induced at the leading edge, where the total velocity is expressed as $\vec{V}+\vec{v}_t$. As a result, the effective attack angle on the windward side, $\alpha_{e,W}$, is decreased, i.e., $\alpha_{e,W}<\alpha$.

On the other hand, on the leeward side, the effective attack angle $\alpha_{e,L}$ is increased. Due to this difference, the pressure distribution on the upper surface is subject to change as the rotation increases.

Near the apex, there exists a case that v_t becomes

small, because the value of local span b_x is small there. Consequently, the effect of rotation angle becomes rather small. This is confirmed by a large ΔC_p region produced near the leading edge on the windward side around the apex.

3.2.2 The case of α=30deg

Figure 9 shows distributions of ΔC_p, i.e., the pressure difference between the upper and lower wing surfaces, at α=30deg for two sideslip angles: β=0 and 10deg.

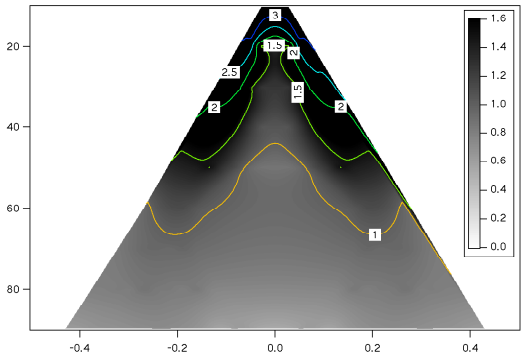

(a) β=0deg

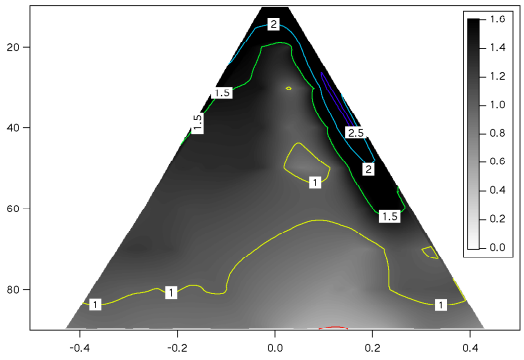

(b) β=10deg

Fig. 9 Distribution of pressure difference between upper and lower wing surfaces at α=30deg in case of no rotation

As shown in Fig. 9(a), a large ΔC_p region exists near the leading edge from the apex to x/c=0.4, and the aerodynamic force effects on the wing are symmetric between windward and leeward sides. Therefore, no rotation can take place.

In the case of α=30deg, the trend is opposite to the case of α=10deg. Figure 9(b) shows the values of ΔC_p on the leeward side is larger than that on the windward side. This asymmetric aerodynamic force distribution causes the wing to rotate.

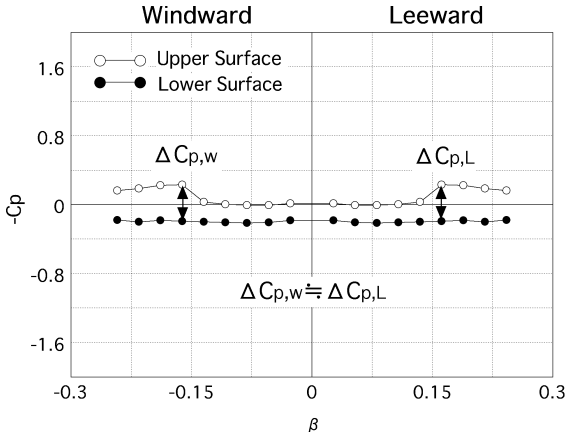

(a) β=0deg

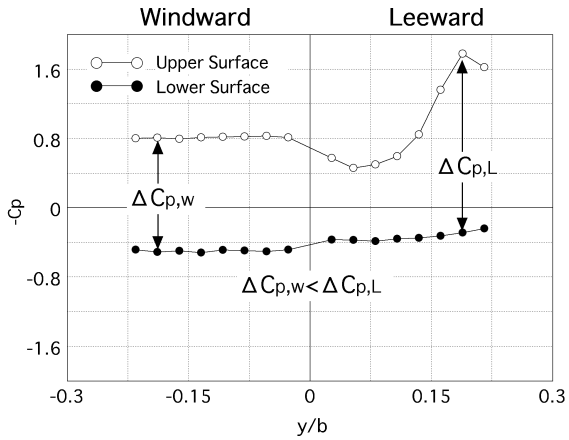

(b) β=10deg

Fig. 10 Spanwise pressure distribution at x/c=0.5 for α=30deg

Figure 10 shows spanwise pressure distributions at x/c=0.5 on the upper and lower wing surfaces. Symmetric low-pressure regions exist near the leading edges (see Fig. 10(a)). This is due to leading edge separation vortices.

From Fig. 10(b), it can be observed that by sideslipping, the upper surface pressures on the leeward side become lower than those on the windward side. Thus, sideslipping can decrease the pressures on the upper surface of the leeward side. Consequently, the effects of aerodynamic force on

the wing become asymmetric, which drives the wing.

At α=10deg, by sideslipping, pressure decreases on the upper surface of windward side, while at α=30deg, this occurs on the leeward side. To clarify the reason for this difference, flow visualization was conducted by a smoke wire method for the flow over the upper surface.

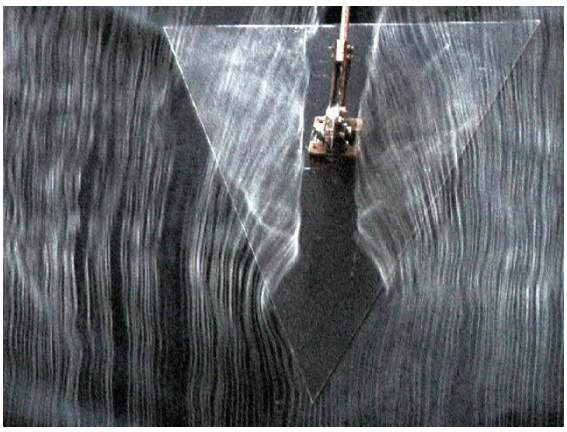

(a) α=30deg, β=0deg

(b) α=30deg, β=10deg

Fig. 11 Flow visualization on upper surface

From Fig. 11(a), we can see a pair of symmetric leading edge separation vortices in the case without sideslipping (β=0deg). On the other hand, it is observed from Fig. 11(b) that the vortex on the leeward side breaks down in the case of sideslipping (β=10deg). These results of flow visualization confirm that the pressures on the upper surface increases on the windward side and decrease on the leeward side.

A change of effective swept back angle, Λ_{eff}, seems to play an important role in producing a leading edge vortex. By sideslipping, Λ_{eff} increases on the windward side, whereas it decreases on the leeward side. As a result, on the windward side the leading edge vortex becomes unstable and its breakdown is promoted. On the contrary on the leeward side the vortex becomes stable.

At α=30deg, S_p is 3.5 times as large as the case of α=10deg. The degree of being asymmetric in aerodynamic force distribution between windward and leeward sides becomes large, so that at α=30deg the vortex on the windward side breaks down, although the vortex exists on both sides at α=10deg.

If this asymmetric force distribution could be kept, the wing rotation number would continue to increase up to infinity. However, in fact, the wing rotates at a certain equilibrium rotation number. To examine this mechanism, pressure was measured on the rotating wing, the results of which are shown in Fig. 12.

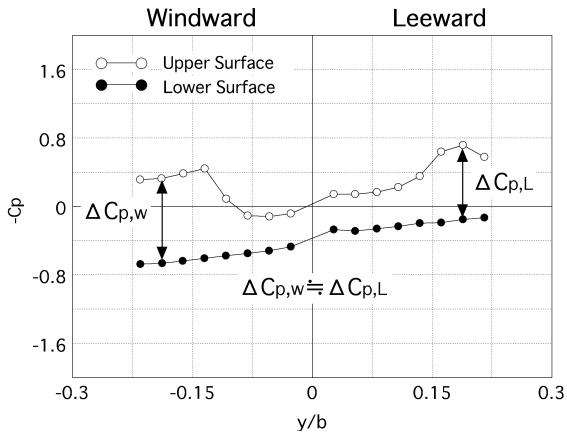

Fig. 12 Pressure distributions in the spanwise direction at x/c=0.5:
. α=30deg, β=10deg, and Sp=0.35

Figure 12 shows pressure distributions in the spanwise direction on the upper and lower surfaces at x/c=0.5, where α=30deg, and β=10deg, and S_p =0.35. In this figure, it is seen that wing rotation can decrease the pressures on the leeward side. Thus the

pressure difference between upper and lower surfaces becomes nearly symmetric by the wing rotation. The reason for this change has been described in Fig.8.

3.2.3 The case of α=50deg

Figure 13(a) shows the spanwise pressure distributions at x/c=0.5 for α=50deg with no sideslip. In this case aerodynamic force effects on the wing is symmetric, which never causes wing rotation. It is also clear that the flow on the upper surface fully separates, because the values of Cp there take about –0.5.

Figure 13(b) shows the pressure distributions with sideslip (β=10deg). In this case the aerodynamic force becomes asymmetric, so that rotation occurs. Sideslip does not affect the pressure distribution on the upper surface. However, pressure increases on the lower surface of the windward side. Thus, the wing rotates.

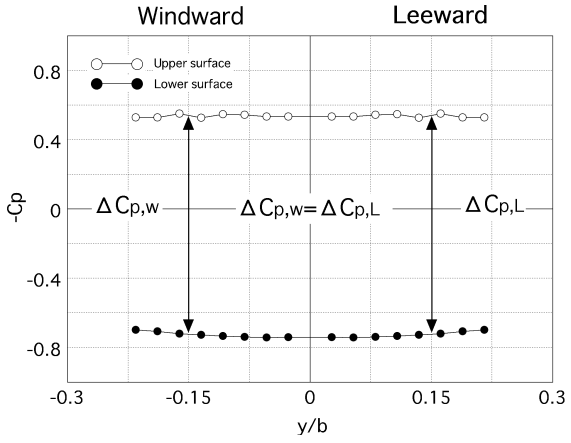

(a) β=0deg

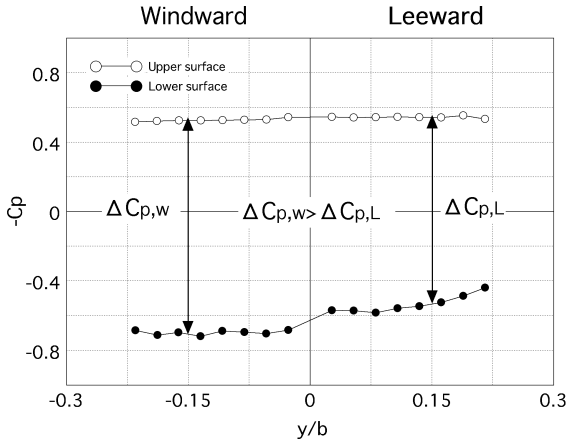

(b) β=10deg

Fig.13 Spanwise pressure distribution at x/c=0.5 for α=50deg

4. CONCLUSION

•At α=10deg with sideslipping, pressure decreases on the windward side and increases on the leeward side. This creates an asymmetric aerodynamic force distribution between each wing-half, which causes the wing to rotate.

•The vortex breakdown on the windward wing-half at α=30deg with sideslipping, changes the pattern in pressure distribution in such a way that the direction of the rotation becomes opposite to that at α=10deg.

•Wing rotation changes the effective attack angle, so that the asymmetry of pressure distribution is suppressed. Thus the wing rotation becomes equilibrium.

•A correlation was confirmed from the visualization between pressure distributions on the wing upper surface and leading edge separation vortices.

•In the post stall case (α=50deg), wing rotates in the same direction as the case of α=10deg, though the rotation speed is negligible.

REFERENCES

[1] S. H. Scher: Effect of 40° Sweepback on the Spin and Recovery Characteristics of a 1/25 Scale Model of a Typical Fighter-type Airplane as Determined by Free-spinning-tunnel Tests, NACA TN1256, 1947.

[2] M. Knight: Wind Tunnel Tests on Autorotation and The "FLAT SPIN", NACA Report No.273, 1927, pp.343-351.

[3] C. J. Wenzinger and T. A. Harris: The Vertical Wind Tunnel of the National Advisory Committee for Aeronautics, NACA Report No. 387, 1931, pp.449-506.

[4] M. J. Bamber: Aerodynamic Rolling and Yawing Moments Produced by Floating Wing-tip Ailerons, as Measured by the Spinning Balance, NACA TN 493, 1934.

[5] N. F. Scudder and M. P. Miller: The Nature of Air

Flow about the Tail of an Airplane in a Spin, NACA TN 421, 1932.

[6] R. W. Stone, Jr. and S. M. Burk, Jr.: Effect of Horizontal-tail Position on the Hinge Moments of an Unbalanced Rudder in Attitudes Simulating Spin Conditions, NACA TN 1337, 1947.

[7] M. J. Bamber: Aerodynamic Effects of a Split Flap on the Spinning Characteristics of a Monoplane Model, NACA TN 515, 1934.

[8] T. Berman: Comparison of Model and Full-scale Spin Test Results for 60 Airplane Designs, NACA TN 2134, 1950.

[9] L. J. Gale and I. P. Jones, Jr.: Effects of Anti-spin Fillets and Dorsal Fins on the Spin and Recovery Characteristics of Airplanes as Determined from Free-spinning-tunnel Tests, NACA TN 1779, 1948.

[10] T. Yamada, M. D. Mamun and Y. Nakamura: Analysis and Control of the Flow Field around Spinning Flat Plate Wing, 39th AIAA Aerospace Sciences Meeting and Exhibit, AIAA-2001-0692, 2001.